

A Genetic Algorithm Approach to Probing the Evolution of Self-Organized Nanostructured Systems

Peter Siepmann,[†] Christopher P. Martin,[‡] Ioan Vancea,[§] Philip J. Moriarty,[‡] and Natalio Krasnogor^{*,†}

School of Computer Science & IT, The University of Nottingham, Nottingham NG7 2RD, U.K., The School of Physics & Astronomy, The University of Nottingham, Nottingham NG7 2RD, U.K., and Max-Planck-Institut für Physik Komplexer Systeme, Nöthnitzer Strasse 38, 01187 Dresden, Germany

Received April 2, 2007; Revised Manuscript Received May 11, 2007

ABSTRACT

We present a new methodology, based on a combination of genetic algorithms and image morphometry, for matching the outcome of a Monte Carlo simulation to experimental observations of a far-from-equilibrium nanosystem. The Monte Carlo model used simulates a colloidal solution of nanoparticles drying on a solid substrate and has previously been shown to produce patterns very similar to those observed experimentally. Our approach enables the broad parameter space associated with simulated nanoparticle self-organization to be searched effectively for a given experimental target morphology.

Complex systems in chemistry, physics, biology, ecology, economics, computer science, and beyond have often been simulated using cellular automata^{1,2} and the closely related lattice gas model technique.³ Both approaches are appealing modeling paradigms not only because they allow for a piecemeal specification of the laws that govern a given system's dynamics but also because they are intrinsically distributed tools amenable to computational parallelization. However, due to the complex nature of the processes that are simulated with these methods, it is not always possible to analytically derive specific values for the many model parameters that control their time–space evolution. This problem gets more insidious when the intention is for the simulation to quantitatively match observations made in the laboratory of experiments where the underlying physics is not wholly understood. Importantly, however, identifying regions of parameter space which produce good agreement with experiment can provide significant insight into the key physicochemical processes underlying the self-organization of the system.

In this Letter we describe how the combination of a Monte Carlo model^{4,5} with a genetic algorithm (GA)⁶ can be used to tune the evolution of a simulated self-organizing nanoscale system toward a predefined nonequilibrium morphology. The prototype system we have chosen—a colloidal solution of Au nanoparticles adsorbed on a substrate—not only produces a striking array of complex nonequilibrium patterns but has

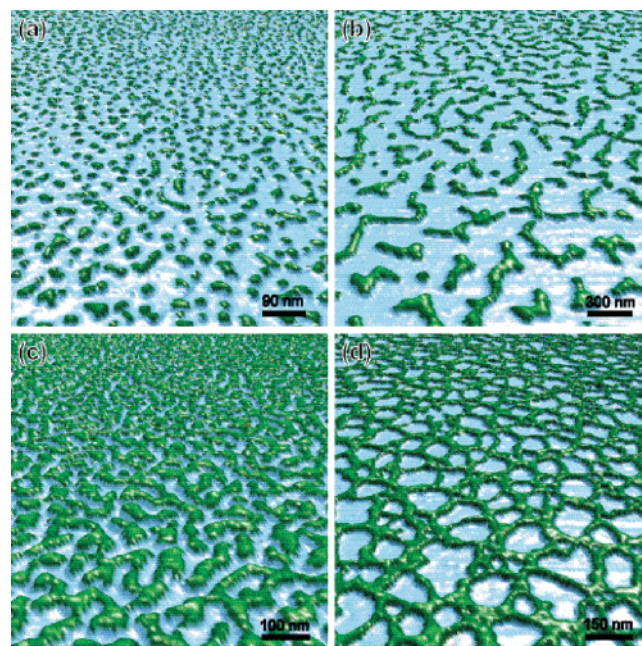


Figure 1. Three-dimensionally-rendered atomic force microscope images showing four of the morphologies that are commonly observed in our experiments. These are formed by spin-casting solutions of ~ 2 nm diameter thiol-passivated gold nanoparticles onto silicon substrates. With increasing solution concentration from (a–d), we observe (a) isolated droplets, (b) “wormlike” domains, (c) interconnected labyrinthine patterns, and (d) cellular networks.

previously been shown^{4,5} to be remarkably well-described by a relatively simple Monte Carlo code. Image morphom-

[†] School of Computer Science & IT, The University of Nottingham.

[‡] The School of Physics & Astronomy, The University of Nottingham.

[§] Max-Planck-Institut für Physik Komplexer Systeme.

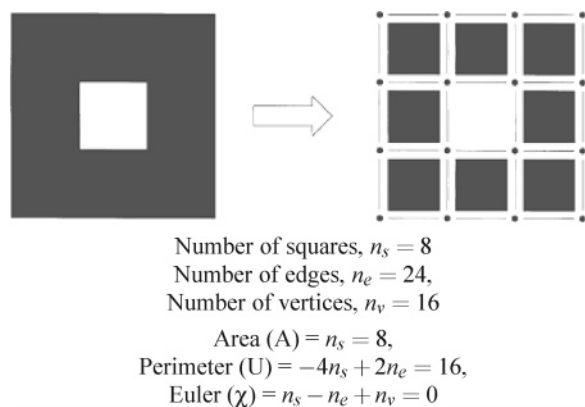


Figure 2. Calculation of the 2D Minkowski functionals that form the basis of the fitness function in the genetic algorithm.⁷

```

while (stopping condition not fulfilled)
  parents = select parents from population
  with a defined probability
  'mate' the parents to form (usually) two children
else
  children = parents
  with a defined probability
  mutate children
  insert children into population
  evaluate and cull population

```

(a) Pseudo-code

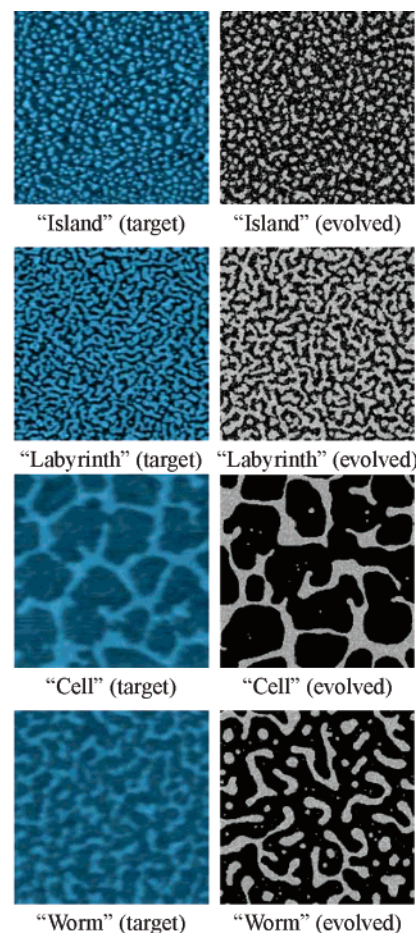
Parent selection: roulette wheel
 Crossover operator: uniform
 Probability of crossover: 0.7
 Mutation operator: BCG²⁶
 Mutation rate: 0.3
 Stopping condition: after 100 generations
 Replacement strategy: $(\mu + \lambda)$, with $\mu = 16$ and $\lambda = 8$

(b) GA system parameters (where μ represents the population size and λ the number of offspring produced in each generation)

Figure 3. Genetic algorithm details.

46 etry—specifically, Minkowski functional analysis⁷—is used
 47 as the basis of the fitness function for the GA. Evolved
 48 simulation parameters produce simulated nanoparticle pat-
 49 terns which closely match the target images taken from
 50 experimental data and replicate a number of morphological
 51 families. Our results provide an important bridge between
 52 simulation and experiment in the study of self-organizing
 53 nanostructured systems and, moreover, bring us closer to the
 54 concept of software control of matter.⁸

55 When deposited onto a solid substrate, colloidal nanopar-
 56 ticles self-organize into a variety of complex patterns^{4,5,9–13}
 57 driven in many cases by the evaporative dewetting of the
 58 solvent. The system of interest in this Letter, namely, Au
 59 nanoparticles in toluene deposited onto a native oxide-
 60 terminated Si(111) substrate, has been described at length
 61 in a number of earlier papers^{5,10,13,14} and here we therefore
 62 include only a brief description of the patterns formed. Figure
 63 1 shows a subset of the different morphologies obtained.
 64 These depend on a number of factors including nanoparticle
 65 concentration, the nature of the solvent and substrate (e.g.,



Target	A_{target}	$A_{evolved}$	A_{error}	U_{target}	$U_{evolved}$	U_{error}	χ_{target}	$\chi_{evolved}$	χ_{error}
Island	304862	308170	1.05%	72512	72198	0.43%	632	596	5.70%
Labyrinth	516669	508958	1.49%	77984	77502	0.62%	114	147	28.95%
Cell	305642	258304	15.50%	18588	24050	29.38%	5	2	60%
Worm	301378	302338	0.32%	32198	34610	7.49%	88	110	25%

Figure 4. Evolved patterns using the Minkowski functional-based fitness function. The left column shows the target, i.e., experimental, images. The right column shows self-organized patterns mimicking the experimental data. These patterns were evolved using the evolutionary algorithm described in the main text. The table shows the specific Minkowski values for the area (A), perimeter (U), and Euler characteristic (χ) for both the experimental target and evolved images as well as the discrepancy, i.e., % error, between the two.

wettability), and the length of the thiol groups used to
 66 passivate the gold particles. Understanding the physical
 67 processes that govern the self-organization of patterns like
 68 those shown in Figure 1 is an area of intense research where
 69 the interplay of simulation and experiment plays a pivotal
 70 role.
 71

72 Our simulations^{5,15} are based on a two-dimensional Monte
 73 Carlo (Metropolis algorithm) model introduced by Rabani
 74 et al.⁴ The solvent is represented as an array of cells on a
 75 square grid, each of which represents 1 nm², and can have
 76 a value of either 1 or 0 to represent liquid or vapor,
 77 respectively. Each gold nanoparticle occupies an area of 3
 78 \times 3 cells, and liquid is excluded from the sites where a
 79 particle is present. The simulation proceeds by two pro-
 80 cesses: the evaporation (and recondensation) of solvent and

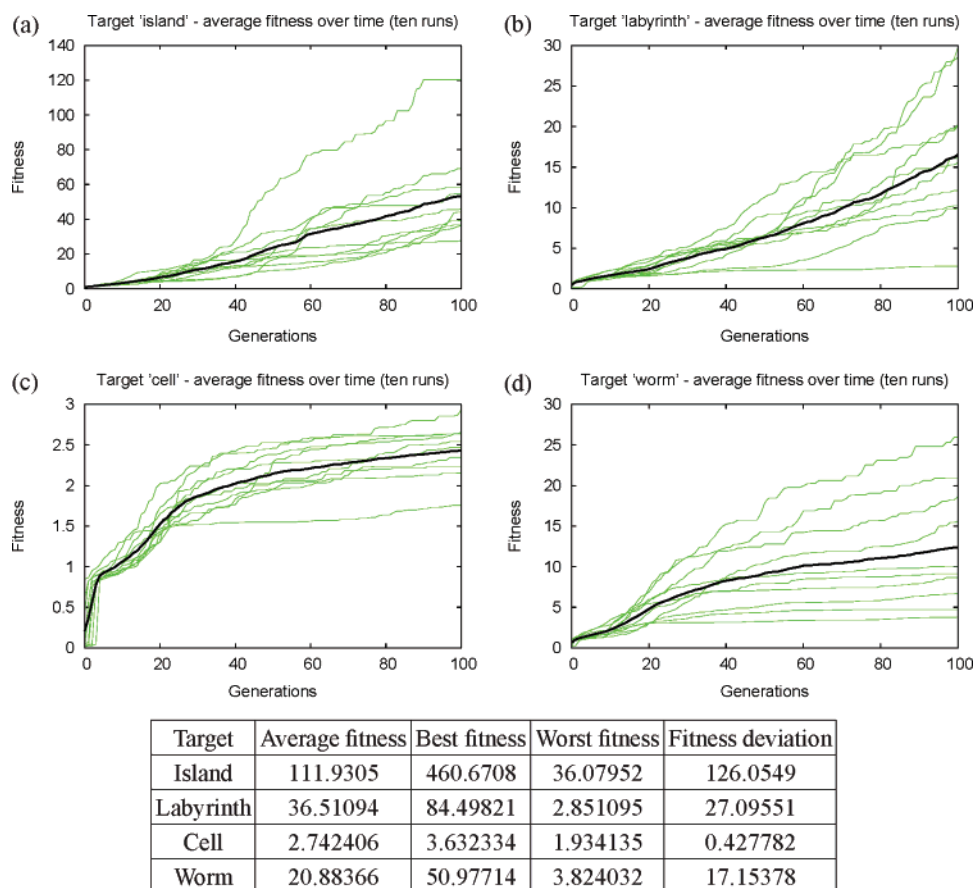


Figure 5. Population dynamics of the genetic algorithm. Each experimental image was used as a target in ten independent runs of the GA. Parts a–d show the average population fitness as a function of time (“generations”) of each run as well as the average evolution (dark line). The table shows, for each experimental target, details of the fitness achieved by the winning individual in each of the ten runs.

81 the random walks of nanoparticles. The Metropolis algorithm
82 is governed by the following equations

$$P_{\text{accept}} = \min\left(1, \exp\left(\frac{-\Delta H}{k_B T}\right)\right) \quad (1)$$

$$H = -\epsilon_l \sum_{\langle i,j \rangle} l_i l_j - \epsilon_n \sum_{\langle i,j \rangle} n_i n_j - \epsilon_{nl} \sum_{\langle i,j \rangle} n_i l_j - \mu \sum_i l_i \quad (2)$$

83 where p_{accept} represents the probability of acceptance of an
84 event, ϵ_l , ϵ_n , and ϵ_{nl} determine the liquid–liquid, nanopar-
85 ticle–nanoparticle, and nanoparticle–liquid interactions,
86 respectively, and μ is the chemical potential of the liquid,
87 which defines its equilibrium state.¹⁵ These parameters
88 determine the nature of the pattern formed as output.

89 In order to program the simulated self-organized patterns
90 to match as closely as possible those observed experimen-
91 tally, we couple the simulator to a genetic algorithm that
92 will tune these parameters. GAs are the mainstay of
93 evolutionary computation and one of the most powerful and
94 widely used methods in the optimization and machine-
95 learning toolbox. They are particularly suited to optimization
96 problems involving very large search spaces and/or complex
97 objective functions which are not amenable to traditional
98 numerical analysis. First proposed in the 1970s by John
99 Holland,¹⁶ GAs have earned great popularity both for their

conceptual simplicity and power, as exemplified in a great
many practical applications,^{17–22} and for their theoretical
foundations.^{23–25} A genetic algorithm maintains a set of
vectors, called a population of individuals, where each vector
represents a particular set of input parameters for the
simulator. Each vector is passed onto the simulator and the
resulting self-organized pattern compared against the ex-
perimental target, evaluated, and assigned a “fitness” value.
Fit individuals “breed” preferentially. Thus good traits
(parameters) present in specific vectors accumulate and, over
time, the average quality of the population increases.

In order to coerce the Monte Carlo simulator into produc-
ing a particular morphology, a method of measuring similar-
ity between self-organized patterns must be used. In this
paper we employ Minkowski functionals.⁷ These characterize
a binary pattern in terms of area, perimeter, and Euler
characteristic (a measure of connectivity) (see Figure 2). The
objective function that the GA is set to minimize is derived
by taking the root mean squared error (RMSE) between the
target Minkowski values and those derived from the evolved
patterns. Hence the fitness of an individual can be seen as
the reciprocal of this RMSE value (as plotted in Figure 5).
As the simulation is intrinsically stochastic, each individual,
i.e., parameter vector, must be evaluated a number of times,
hence the use of mean errors. Also, as each Minkowski
functional can take values over widely different intervals,

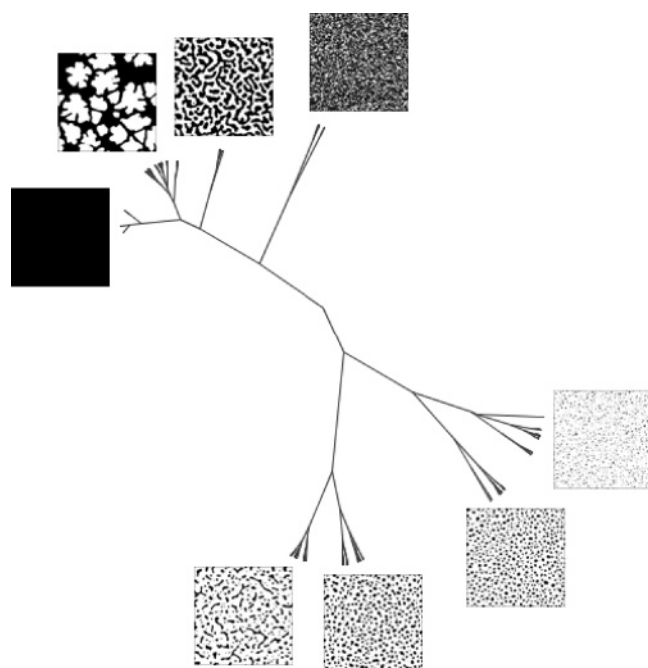


Figure 6. A partial depiction of the logarithmic cluster tree for the 256-piece dataset.

126 we scale each functional to the [0,1] interval so as to give
 127 each of them equal weighting within the fitness function.
 128 The GA is initialized with a randomly generated population,

129 i.e., multiset, of vectors and we let the evolutionary process
 130 take its course for a number of generations. A generic GA
 131 pseudocode, along with parameters from our system, is
 132 shown in Figure 3.

133 To test the methodology described above, we defined a set
 134 of four patterns, each demonstrating different morphological
 135 families, taken from *experimental images* (see Figure 4).
 136 These four patterns were the “targets” that the GA needed
 137 to reverse engineer by finding a suitable set of parameters
 138 for the MC simulator. For any of the given targets, the GA
 139 was run for 100 generations using a population of 20
 140 individuals. Each individual comprised a candidate parameter
 141 set for the MC simulator. On each target pattern we run the
 142 GA ten times.

143 In every case, the simulator was run for 1000 Monte Carlo
 144 cycles. Figure 4 shows representative results from the GA
 145 runs that are characterized by the striking similarity to their
 146 respective targets; the results for the island and labyrinth
 147 targets are particularly good and taking into account that both
 148 the experimental and simulated patterns arise from a
 149 stochastic process (i.e., for a given parameter set two distinct
 150 runs will produce similar yet not identical behaviors) the cell
 151 and worm patterns are also remarkably close to their
 152 experimental objective.

153 As shown in the evolution graphs and the statistics shown
 154 in Figure 5, each run followed a similar evolutionary
 155 trajectory. A good (i.e., visually acceptable) result was

Family name	Characteristics	Example	Number of samples
Cell	Highly connected, large length scale		17
Island	Large number of unconnected, small, regular clusters		71
Labyrinth	Highly connected, small length scale		24
Worm	Disconnected, larger non-regular clusters		14
Indiscernible	No spatially correlated pattern visible		60
No pattern	Completely black (i.e., solvent saturated)		63
Unusual	Other novel patterns, including fingering morphologies ³⁰		7

Figure 7. Table illustrating the size of the different morphological families found in the dataset. Families containing a larger number of representative patterns are deemed more designable as it is easier for the GA to find a parameter set realizing the pattern.

156 obtained in each of the ten runs performed for each target,
 157 despite the often large standard deviations. Indeed, even for
 158 the “worst” runs, although the numerical fitness is substan-
 159 tially lower than average, the result was still visually
 160 acceptable (though not as convincing, of course, as the
 161 pattern evolved in the “best” run). This surprising feature
 162 can be best explained by performing a detailed analysis of
 163 the Minkowski-based fitness function as we recently pro-
 164 posed in ref 20.

165 We defined a dataset comprising 256 sample images
 166 representing a cross section of the entire range of simulation
 167 parameters. Clustering this dataset using the Minkowski-
 168 based fitness function taken as a similarity measure results
 169 in a hierarchical tree that organizes simulation results based
 170 on their topological distances. Figure 6 shows the tree we
 171 obtain for our dataset. Note how each of the 14 main clusters
 172 represents a particular type of morphology. There are some
 173 clusters, such as 1 and 4 that look visually very similar, yet
 174 are quite far apart in the tree; this draws attention to the fact
 175 that the Minkowski functionals are often more sensitive than
 176 human vision, i.e., two images that look similar can have
 177 quite different Minkowski values. This result provides an
 178 explanation for the observation made above that even for
 179 results with a numerical fitness substantially lower than
 180 average, the result was still visually acceptable.

181 Particularly interesting to note is that the cluster analysis
 182 shows that the search space can be partitioned into a number
 183 of “families” of morphological likeness. A simple manual
 184 (visual) classification of these into morphological families
 185 in Figure 7 shows the relative size of each class. We note
 186 that in general, those targets scoring higher fitness tend to
 187 be members of the larger families, that is, these patterns are
 188 more *designable*.²⁷ This supports the observation from our
 189 results above that the evolution of, e.g., the “island” target,
 190 achieved much higher fitnesses than the other three targets,
 191 while the “cell” target produced relatively low values.
 192 Interestingly, it has been argued that designability plays a
 193 key role in the evolution of proteins.^{28,29} An analogy can be
 194 made: as it is the case for proteins where a complex sequence
 195 \rightarrow structure \rightarrow function mapping exists and is molded by
 196 natural selection, the self-organized nanostructures studied
 197 in this paper also present a similar mapping albeit “imple-
 198 mented” in a different way. That is, the nanosystems studied
 199 here can be thought as obeying the following mapping
 200 sequence: experimental conditions/MC parameters \rightarrow struc-
 201 ture: self-organized pattern \rightarrow function. We argue that future
 202 implementations of intelligent self-organized surfaces could
 203 use a process of artificial selection such as that presented in
 204 this paper in order to evolve toward target *function*, rather
 205 than *structure* as done in this paper, if the desired functions
 206 were to be embodied into the more designable structures.

207 This work has presented evolutionary computation as a
 208 method for designing target morphologies of self-organizing
 209 nanostructured systems. We have used Minkowski function-
 210 als to direct the evolution in search of simulated patterns
 211 that closely mimic those observed experimentally. The
 212 simulation is also able to produce a number of patterns that
 213 are more uncommon in experiments, such as branched

structures that are reminiscent of viscous fingering.^{31,32} The
 obvious, albeit extremely challenging, next step is to couple
 the GA directly to an experiment rather than a simulator, in
 a fashion similar to the research currently being explored
 by the CHELLnet project.³³

Acknowledgment. The authors gratefully acknowledge
 the support of Marie Curie Actions through their funding of
 Grant MRTN-CT-2004005728 and the EPSRC through the
 funding of Grants EP/D021847/1 and EP/E017215/1. C.P.M.
 was supported by an EPSRC DTA award.

References

- (1) Toffoli, T.; Margolus, N. *Cellular automata machines - a new environment for modelling*; MIT Press: Cambridge, MA, 1987.
- (2) Chopard, B.; Droz, M. *Cellular automata modeling of physical systems*; Cambridge University Press: Cambridge, 1998.
- (3) *Santa Fe studies in the science of Complexity*; Dooler, G., Ed.; Addison Wesley Longman Publishers: Reading, MA, 1990.
- (4) Rabani, E.; Reichman, D. R.; Geissler, P. L.; Brus, L. E. *Nature* **2003**, *426*, 271–274.
- (5) Martin, C. P.; Blunt, M. O.; Moriarty, P. *Nano Lett.* **2004**, *4*, 2389–2392.
- (6) Goldberg, D. E. *Genetic Algorithms in Search, Optimization and Machine Learning*; Addison-Wesley Longman Publishing Co., Inc.: Boston, MA, 1989.
- (7) Michielsen, K.; de Raedt, H. *Phys. Rep.* **347**, **2001**, 461–538.
- (8) Pollack, J. B.; Lipson, H.; Ficici, S.; Funes, P.; Hornby, G.; Watson, R. In *Evolvable Systems: from biology to hardware; proceedings of the third international conference (ICES 2000)*; Miller, J., et al., Eds.; Lecture Notes in Computer Science; Springer: Berlin, 2000; pp 175–186.
- (9) Ge, G.; Brus, L. J. *Phys. Chem. B* **2000**, *104*, 9573–9575.
- (10) Moriarty, P.; Taylor, M. D. R.; Brust, M. *Phys. Rev. Lett.* **2002**, *89*.
- (11) Narayanan, S.; Wang, J.; Lin, X.-M. *Phys. Rev. Lett.* **2004**, *93*.
- (12) Bigioni, T. P.; Lin, X.-M.; Nguyen, T. T.; Corwin, E. I.; Witten, T. A.; Jaeger, H. M. *Nat. Mater.* **2006**, *5*.
- (13) Blunt, M. O.; Martin, C. P.; Ahola-Tuomi, M.; Pauliac-Vaujour, E.; Sharp, P.; Nativo, P.; Brust, M.; Moriarty, P. J. *Nat. Nanotechnol.* **2007**, *2*, 167.
- (14) Blunt, M. O.; Suvakov, M.; Pulizzi, F.; Martin, C. P.; Pauliac-Vaujour, E.; Stannard, A.; Rushforth, A. W.; Tadic, B.; Moriarty, P. J. *Nano Lett.* **2007**, *7*, 855.
- (15) Martin, C. P.; Blunt, M. O.; Pauliac-Vaujour, E.; Vancea, I.; Thiele, U.; Moriarty, P. Unpublished. We have recently found that by using a simple modification to the chemical potential term in eq 2, it is possible to simulate classes of patterns observed experimentally but not reproduced by the standard Rabani et al. algorithm. Here we use only the original Rabani et al. algorithm⁴ modified as described by Martin et al.⁵ to include next-nearest-neighbor interactions.
- (16) Holland, J. H. *Adaptation in Natural and Artificial Systems: An Introductory Analysis with Applications to Biology, Control, and Artificial Intelligence*; University of Michigan Press: Ann Arbor, MI, 1975.
- (17) Harding, S.; Miller, J.; Rietman, E. *IEEE Trans. Nanotechnol.* **2005**.
- (18) Thompson. In *Proceedings of the First International Conference on Evolvable Systems*, 1996.
- (19) Mitchell, M.; Crutchfield, J.; Das, R. In *Proceedings of the First International Conference on Evolutionary Computation and its Applications*, 1996.
- (20) Krasnogor, N.; Siepmann, P.; Terrazas, G. In *Proceedings of the Seventh International Conference of Adaptive Computing in Design and Manufacture*, 2006.
- (21) Kruska, J. B. *Proceedings of the American Mathematical Society*, (1), pp 48–50.
- (22) Horn, J. In *Proceedings of IEEE Congress on Evolutionary Computation*, 2005.
- (23) Shapiro, J. L. *Theoretical Aspects of Evolutionary Computing*; Springer: Berlin, 2001; pp 87–108.
- (24) Poli, R.; McPhee, N. F.; Rowe, J. E. *Genetic Programming and Evolvable Machines*, **2004**, *5* (1), 31–70.
- (25) Krasnogor, N.; Smith, J. E. *J. Mathematical Modelling Algorithms*, in press.
- (26) Lozano, M.; Herrera, F.; Krasnogor, N.; Molina, D.

286	(27) Hogg, T. <i>Nanotechnology</i> 1999 , <i>10</i> (3), 300–307(8).		
287	(28) Li, H.; Helling, R.; Tang, C.; Wingreen, N. Emergence of preferred	(32) Pauliac-Vaujour, E.; et al. in preparation.	294
288	structures in a simple model of protein folding. <i>Science</i> 1996 , <i>273</i>	(33) Cronin, L.; Krasnogor, N.; Davis, B. G.; Alexander, C.; Robertson,	295
289	(5275), 666–669.	N.; Steinke, J. H. G.; Schroeder, S. L. M.; Khlobystov, A. N.; Cooper,	296
290	(29) Wong, P.; Frishman, D. Fold designability, distribution, and disease.	G.; Gardner, P.; Siepmann, P. A.; Whitaker, B. J.; Marsh, D. <i>Nat.</i>	297
291	<i>PLoS Comput. Biol.</i> 2006 , <i>2</i> (5).	<i>Biotechnol.</i> October 2006 , <i>24</i> (10).	298
292	(30) Yosef, G.; Rabani, E. <i>J. Phys. Chem B</i> 2006 , <i>110</i> , 20965–20972.		
293	(31) Hele-Shaw, H. S. <i>Nature</i> 1898 , 58.	NL070773M	299